High Temperature Corrosion Test of a Zirconium alloy

Je-Kyun Baek

Department of Nuclear Engineering
Graduate School of UNIST

2015

High Temperature Corrosion Test of a Zirconium alloy

A thesis
submitted to the Graduate School of UNIST
in partial fulfillment of the
requirements for the degree of
Master of Science

Je-Kyun Baek

01. 16. 2015
Approved by

Dong-Seong Sohn

High Temperature Corrosion Test of a Zirconium alloy

Je-Kyun Baek

This certifies that the thesis of Je-Kyun Baek is approved.

01. 16. 2015

Dong-Seong Sohn

Ji Hyun Kim

In Cheol Bang

Abstract

The possibility of breakaway oxidation of zirconium alloy cladding at high temperatures around 1000ºC during small and large LOCA has been a concern in recent years. In March 2014, NRC proposed the revision of the ECCS acceptance criteria which breakaway oxidation was added to the previous criteria: the peak cladding temperature, cladding embrittlement, maximum hydrogen absorption, etc. in recent Federal Register. The standard, 10CFR50.46 which is proposed by NRC requires setting up the breakaway oxidation criterion based on actual performance of the fuel cladding and confirming the criterion by the periodic test of cladding tube which is used in the plant.

High temperature oxidation of zirconium alloy has different trends with the low temperature oxidation because there are several differences between the low and high temperature oxidation. Because the oxidation depends on diffusion of oxygen, hydrogen, electron, and etc., oxidation rate is increased exponentially by increasing of oxidation temperature. Phase transformations of zirconium and their oxide are also concerned at high temperature; zirconium alloy can be received the distinctive phenomena by causing phase transformation.

Zirconium alloy has a passivity of oxidation from the formation of dense oxide layer. The oxidation rate of zirconium alloy is reduced exponentially at first time. But when the zirconium oxide layer is changed into non-protective phase after some moment, oxidation kinetics is turned into linear or exponentially increased through the time. The transition of oxidation kinetics causes surface discoloration and this phenomenon is called as ‘breakaway oxidation’. As mentioned before, the transition of oxidation kinetics is usually faster at higher temperature. But breakaway oxidation can be easily observed at certain points which are 800ºC and 1000ºC not at higher temperature.

In order to simulate LOCA condition which is represented by the high temperature steam oxidation of rapidly heated cladding and subsequent quenching by water, a radiant heating system with the steam and water supply system are used for the test. A radiant heating system that used in the most of LOCA simulation tests, adopts the 4 or 6 line bulbs in order to achieve uniform heating in a circumferential direction. The verification of test equipment should be performed with the sequence of draft regulatory guide which is published by U.S NRC. Axial and circumferential temperature distribution is measured by a specimen with the welded thermocouples and the results of measurement are satisfied with the recommendation in the guide.

The steam supply equipment is one of the important systems for the high temperature oxidation test because the high temperature oxidation test should be conducted in steam ambient. But the initial

steam supply equipment has a problem which is unstable steam flow, so the new steam supply equipment was installed on the system. The new steam supply equipment don't show any unstable steam flow and the steam generation rates of new steam supply equipment were measured by plate-type heat exchanger.

The measurement of weight gain was performed and the results of measurement are compared with the well-established data of ZIRLO which was tested by Westinghouse and ANL. The results of ZIRLO weight gain measurement are consistent with the well-established data and these results are verified the high temperature oxidation test successfully.

The microstructure of ZIRLO after the high temperature oxidation test is confirmed. At the first time, the microstructure of ZIRLO has flat interface between metal and oxide, but wavy metal / oxide interface can be observed in the picture after some moment. Wavy interface between metal and oxide is estimated to the precursor to breakaway oxidation phenomenon and the microstructure after the high temperature oxidation test is shown similar as the most of previous research. Thus, the successful test results are shown in the microstructure.

Contents

List of figures

List of tables

Nomenclature

ANL	Argonne national laboratory
BCC	Body centered cubic
DAS	Data acquisition system
DHC	Delayed hydride cracking
ECCS	Emergency core cooling system
ECR	Equivalent cladding reacted
HCP	Hexagonal closest packing
IR	Infrared
LOCA	Loss of coolant accident
PVDF	Polyvinylidene fluoride
NRC	Nuclear regulatory commission

I. Introduction

1.1 General background

Zirconium alloy is the key component of nuclear thermal reactor such as cladding, pressurized tube, fuel channel, spacer grid, and etc. Because they have a low neutron absorption cross section, good irradiation, physical properties, and etc. When zirconium alloy experiences the high temperature environment with the steam condition in the accident situations, the high temperature oxidation properties of zirconium alloy are shown different oxidation kinetics which is different from normal oxidation kinetics because of the phase transition, oxidation rate, etc.

U.S NRC 10 CFR 50.46(b) [1] specifies criteria that were derived from tests with un-irradiated zirconium alloy cladding. These criteria limit were established in 1973; the peak cladding temperature shouldn't be over 1204ºC and the maximum cladding oxidation shouldn't be over 17% ECR during LOCA. The limits of peak cladding temperature and maximum cladding oxidation prevent cladding from the embrittlement and help the core to stay cool for long term during and after the operation of ECCS [2].

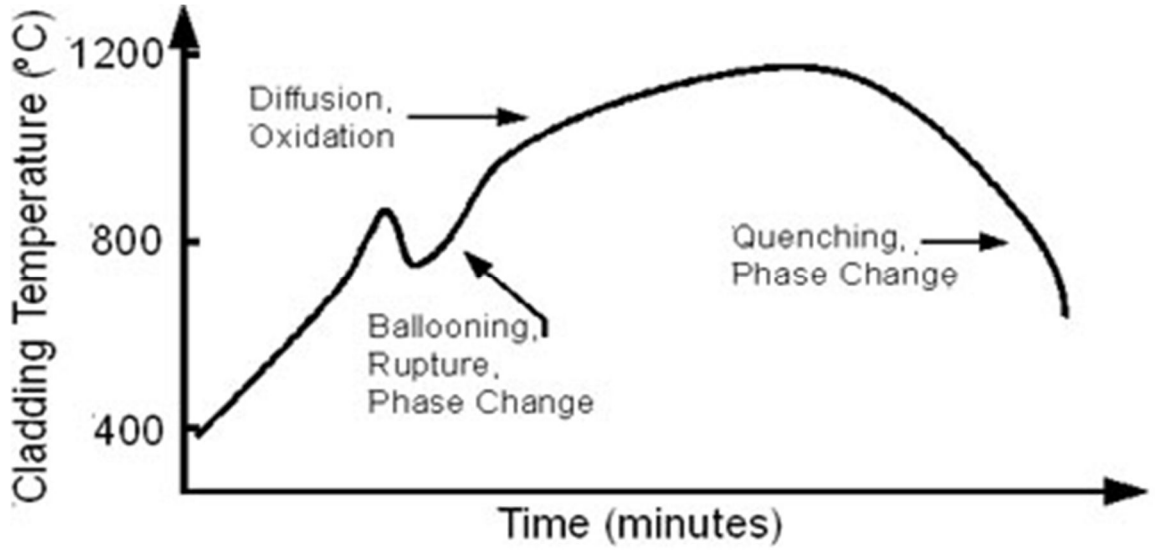

Figure I-1 Schematic of the temperature change of cladding in the LOCA accident [2b]

U.S NRC started a fuel-cladding research program which investigates the behavior of highly irradiated cladding under LOCA condition in 1996. The research program includes several behavior of cladding under LOCA conditions; ballooning strains, flow area reduction, rupture conditions, axial distribution of heat sources, and cladding embrittlement. Especially, the cladding embrittlement is dealt in the paper between these cladding behaviors. One of the cladding embrittlement mechanism which investigated in the research program of the NRC is called as breakaway oxidation[3].

1.2 The goal and scope of this study

Breakaway oxidation can be occurred during the high temperature oxidation test and it is related to the embrittlement of cladding. The high temperature oxidation test and subsequent ductility test are needed to assess the breakaway oxidation phenomenon and the guide of high temperature oxidation and post-quench ductility test was published on 2011. Each the draft regulatory guide 1261 [3], 1262 [4], 1263 [5] includes the contents about the test method of breakaway oxidation, post-quench ductility, and methodology of analytical limits. The only test method and results of breakaway oxidation that the draft regulatory guide 1261 was suggested are written in the paper.

In the following chapter, the previous theories of breakaway oxidation and the literature survey of normal and high temperature oxidation which is conducted with the test of breakaway oxidation are shown in the following chapter. The verification test for breakaway oxidation test has been performed. The results of experiment are compared with the well-established data to identify if it is reliable. Thus, the overall contents in the paper are following; the literature survey, test method, test equipment modification, and test results of verification test.

II. High temperature corrosion of zirconium alloy

2.1 Oxidation of zirconium alloy

2.1.1 Basis of zirconium alloy oxidation

Corrosion between zirconium alloy and water in the nuclear reactor has the embrittlement behavior by hydrogen absorption in the cladding and embrittlement phenomenon is one of the major factors of fuel lifetime limitation. The reactions are oxygen ion oxidized to the oxygen atom and hydrogen ion deoxidized to the hydrogen atom and they are occurred in the zirconium alloy in the nuclear reactor like Figure II-1. The source of oxygen and hydrogen ion come from a little oxygen and hydrogen ion in the water, or decomposed water by high temperature and irradiation environment in the nuclear reactor [6].

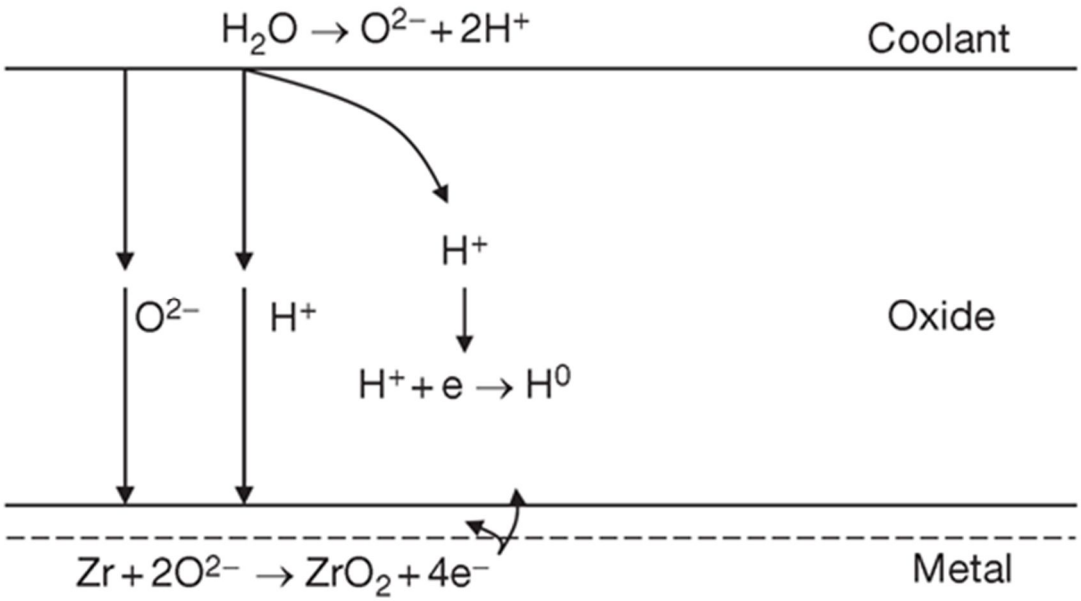

Figure II-1 Schematic of corrosion of zirconium alloys [6]

The movement of oxygen ion, hydrogen ion, and electron is the key which explains these oxidation and reduction. First of all, when an oxygen ion moves to the metal-oxide interface, it forms an oxygen atom by reacting with zirconium. The electrons that produced through the formation of the oxygen

atom diffuse to the oxide layers according to electromagnetic force, and they react with hydrogen ions and form the hydrogen atom. These oxygen and hydrogen atoms form zirconium dioxide or hydride because of their low solubility [6].

2.1.2 Relationship between oxidation rate and temperature

The oxidation of metal is very sensitive to temperature and the graph in the Figure II-2 shows the comparison between the weight gain and temperature of oxidation about Zircaloy-4 during 2500 days in the autoclave. As the graph shows, oxidation rate is increased rapidly by increasing temperature [6-7].

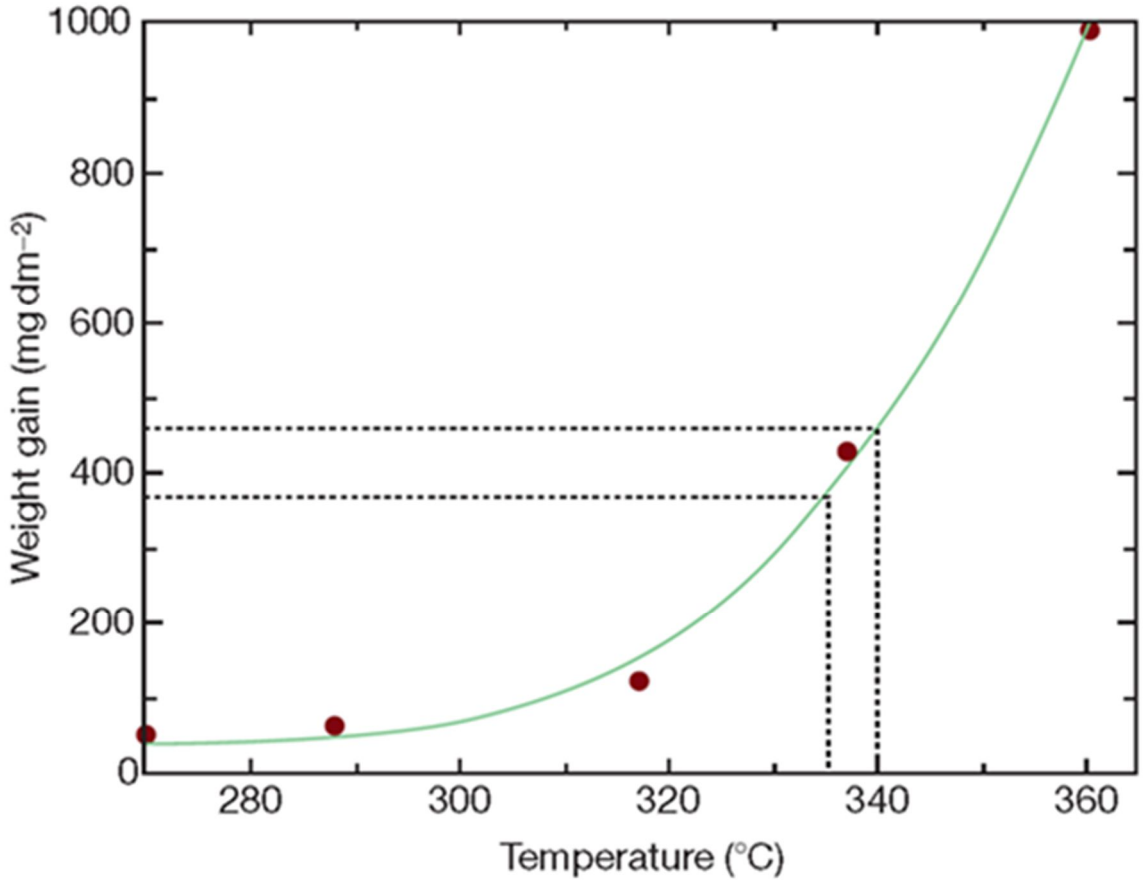

Figure II-2 Temperature effect of oxidation kinetics of Zircaloy-4 [6]

2.1.3 Phase diagram of zirconium-oxygen

Zirconium and their oxide phases are important to understand the behavior of oxidation kinetics. The binary phase diagram of zirconium-oxygen is shown in the left side of Figure II-3 and the pseudo-binary phase diagram is shown in the right side of Figure II-3. The left side of the binary phase diagram shows zirconium phase which has low percentage of oxygen. When percentage of oxygen is over 60at%, oxide phase would be shown.

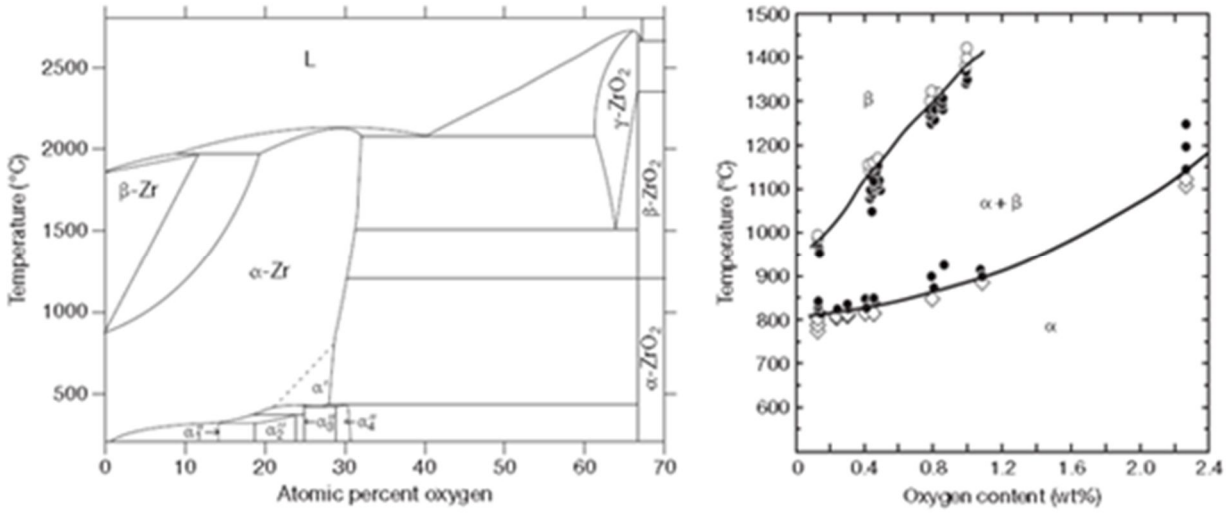

Figure II-3 Zr-O binary phase diagram (left) [8] and pseudo-binary phase diagram (right) [9]

Zirconium phase can be classified into two types; α-Zr which is constructed by hexagonal closest packing (HCP) at low temperature and β-Zr which is constructed by body centered cubic (BCC) at high temperature. Temperature that changes α-Zr into α+β phase is about 800ºC and α+β phase into β-Zr is about 1000ºC. Zirconium oxide phase can be classified into the three types which are from low to high temperature sequences; α-ZrO_2 with monoclinic structure, β-ZrO_2 with tetragonal structure, γ-ZrO_2 with cubic structure [9].

2.1.4 Thermodynamic properties of zirconium-oxide

Most of the compound, including oxide phase, can be verified its stability of compound structure by using the concept of Gibbs free energy. Ellingham/Richardson diagram is the graph of the Gibbs free energy of oxide as Figure II-4.

Spontaneity of the reaction can be determined by Ellingham/Richardson diagram. The red line in the Figure II-4 is the Gibbs free energy which is the reaction that appears when Zr changes into ZrO_2. Oxygen partial pressure, CO/CO_2 ratio or H_2/H_2O ratio should be known to verify spontaneous reaction. The scale on the right side of diagram labeled "Po_2" (Partial pressure of oxygen) is used to determine whether partial pressure of oxygen is stabilized or not when the oxide of metal is produced at a given temperature. When carbon is used as a reducing agent, if the Gibbs free energy of metal should be under the Gibbs free energy that is corresponded to a ratio of CO to CO_2, they would be able to reduce a given oxide. H_2/H_2O ratio is used to the similar perspective with CO/CO_2 ratio. Oxygen partial pressure, CO/CO_2 ratio or H_2/H_2O ratio scale should be selected proper factor according to the reaction form [10].

Zirconium atom is usually reacted with water and forms ZrO_2 and hydrogen. The reaction spontaneously occurs when H_2/H_2O ratio increases higher than red line in the Figure II-4. Gibbs free energy of zirconium at 1000ºC which is most serious temperature of breakaway oxidation is about -860kJ. H_2/H_2O ratio should be higher than 10^9 for the nonspontaneous reaction at 1000ºC, it is very high H_2/H_2O ratio. Of course H_2/H_2O ratio should be higher than 10^9 when the temperature conditions is below 1000ºC and zirconium oxide is expected to be produced spontaneously.

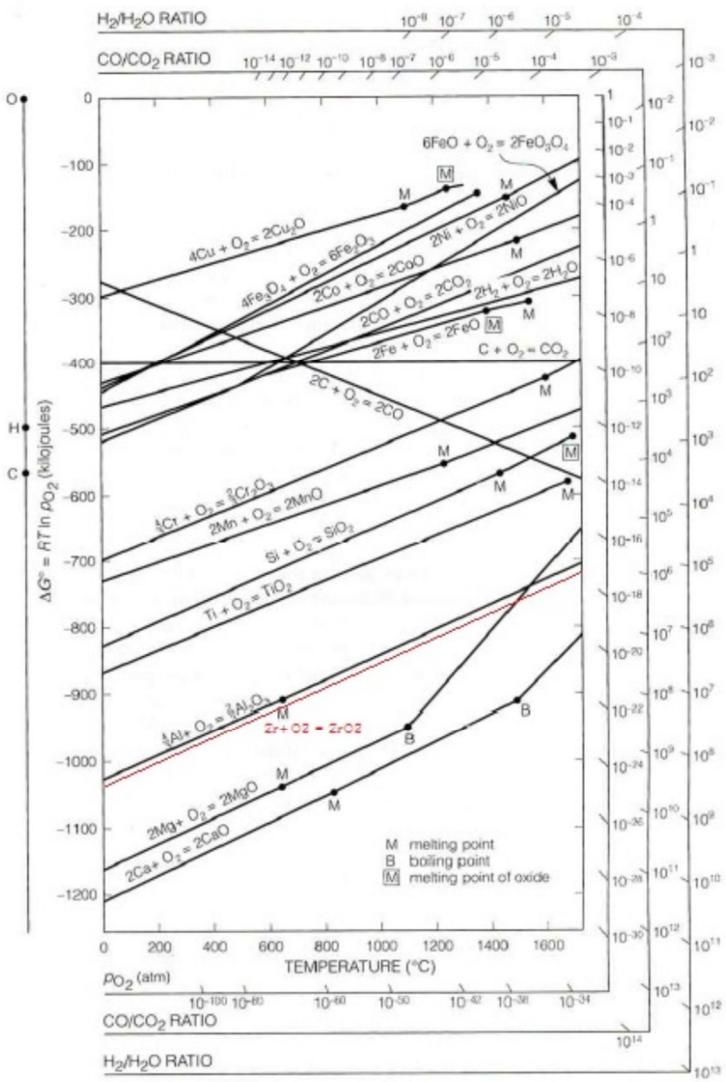

Figure II-4 The ellingham diagram of oxide including zirconium oxide [10-11]

2.2 High temperature corrosion of zirconium alloy

2.2.1 Structure of zirconium alloy after high temperature oxidation

Edge of zirconium alloy is covered by their oxide layer when the zirconium alloy is oxidized at the high temperature, and rim of zirconium metal consists of α-Zr(O) phase which contains a high level of

oxygen contents. There is β layer that is stable at the high temperature over 1000ºC inside of α-Zr(O) layer. The oxygen contents of zirconium (left) and microstructure of zirconium alloy which is observed by microscope (right) at the room temperature after the high temperature oxidation are shown in the Figure II-5. As mentioned before, the right side of Figure II-5 can be observed in a sequence from the outside, oxide – α layer – β layer. This structure is formed because α layer has better stability of oxygen than β layer has. Zirconium alloy experiences quenching because the ECCS injects water in the LOCA situation, quenching water usually uses to the high temperature corrosion test for the similar condition. β layer after quenching cannot have an enough time to become a perfect α layer, they have the properties of both α and β layer. These α layer which have the properties of β layer are named as prior-β layer, finally the structure of zirconium alloy is taken three layers; zirconium dioxide (ZrO2, oxide layer), α-Zr(O), and prior-β layer [9, 12].

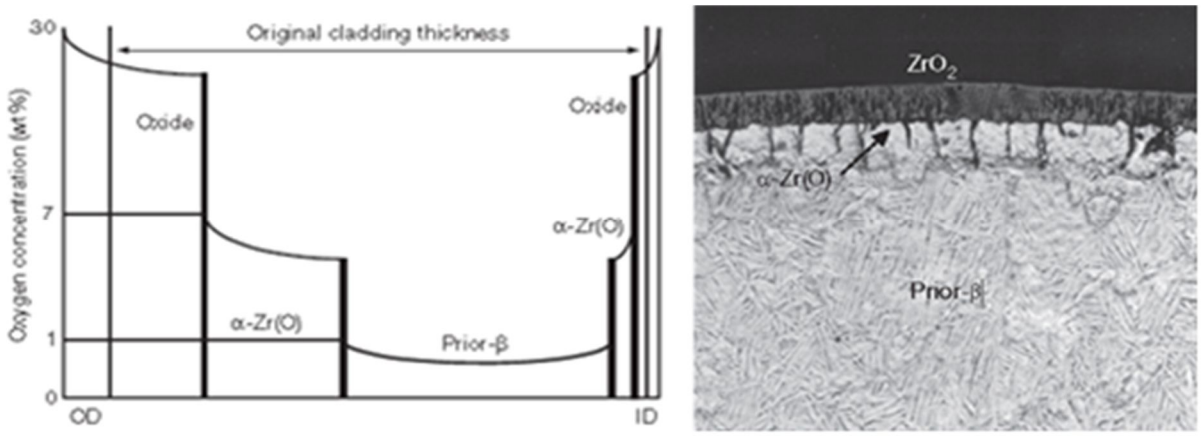

Figure II-5 Radial concentration of oxygen in oxidized zirconium cladding (left) and radial cross-section of Zircaloy cladding oxidized at 1100ºC (right) [9]

The oxide layer and α-Zr(O) layer become thicker with longer oxidation time, these can be confirmed by Figure II-6. Oxidation time is the shortest in the (a) and gets longer to (d), the mark Ⅰ indicates the α-Zr(O) layer which is located between the brown color oxide layer and yellow color

zirconium metal layer. The brown oxide layer and α-Zr(O) layer are thickest in the (d) when oxidation time is longest in the Figure II-6 [13].

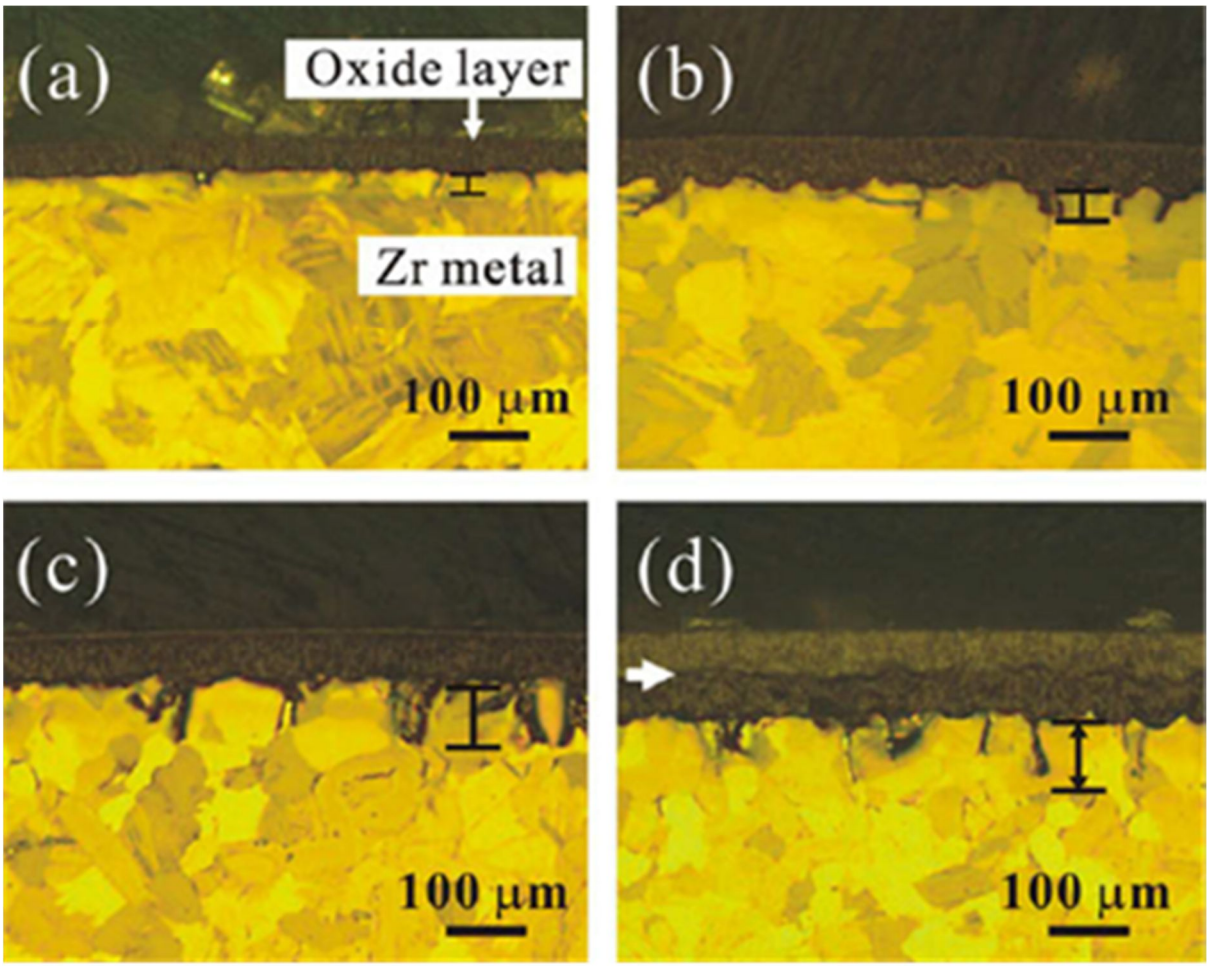

Figure II-6 The optical metallographs of outer surface oxide layers oxidized at 1000 ºC with different oxidation times: (a) 300 s, (b) 2000 s, (c) 3000 s, and (d) 4000 s [13]

2.2.2 Hydrogenation phenomenon of zirconium alloy

Zirconium alloy takes oxide layer during oxidation phenomenon and they absorb hydrogen which is the byproduct of reaction. Zirconium alloy has a very low solubility of hydrogen (about 80wt ppm at 300 ºC and 200wt ppm at 400 ºC, higher solubility can be observed when higher temperature is achieved [6, 14]), hydrogen is reacted with zirconium and formed zirconium hydride. The reaction equation is as the following equation;

$$\mathrm{Zr(H,sln)} + H_2 \rightarrow ZrH_n (n = 1.6\sim2)$$

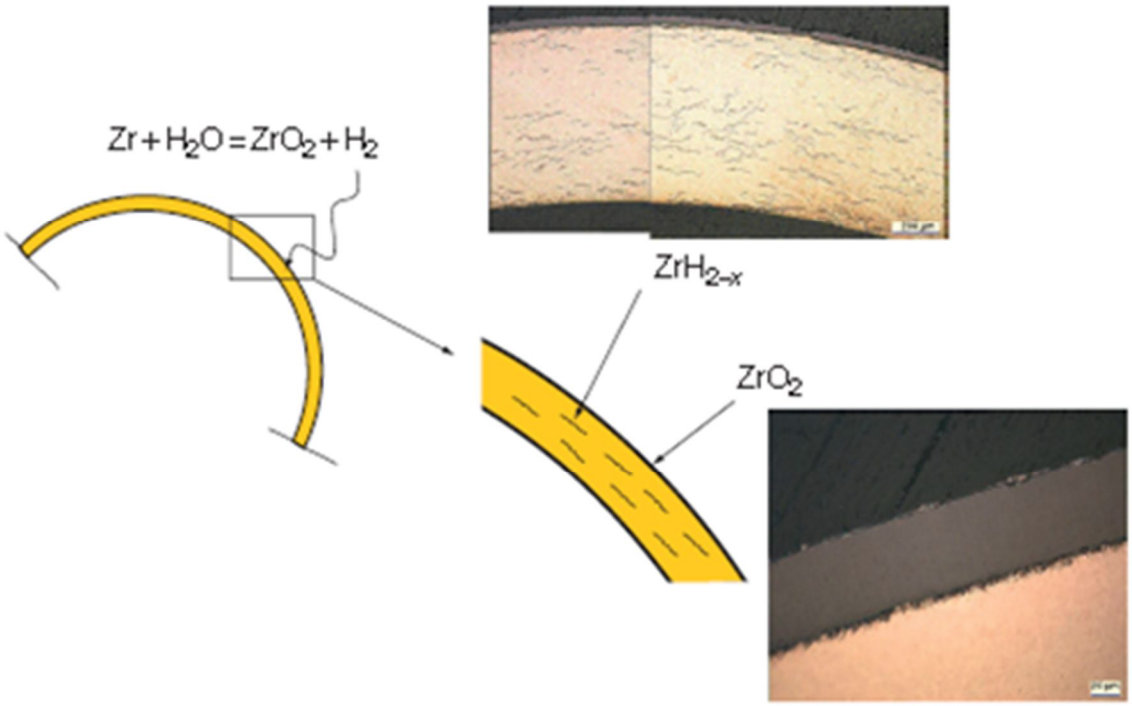

Figure II-7 The formation of uniform oxide layer and hydride precipitation in Zircaloy cladding [6]

Zirconium hydride forms circumferential shape like Figure II-7, zirconium alloy has the following effects to occur in the zirconium cladding when zirconium alloy absorbs hydrogen: hydrogen embrittlement dues to excess hydrogen or its localization into a blister or rim loss of fracture toughness, delay hydride cracking (DHC), acceleration of corrosion and accelaration of irradiation growth [6]. These effects cause the factor of fracture of zirconium and breakaway oxidation is related with the hydrogenation phenomenon.

Relationship between hydrogen contents and oxidation time is shown each zirconium alloy in the left side of Figure II-8, and relationship between thickness of oxide layer and oxidation time is shown in the right side of Figure II-8. HANA-5, 6, Alloy-A(ZIRLO) and Zircaloy-4 are used to test the data on the Figure II-8, ZIRLO and Zircaloy-4 data might be focused on [12b].

All of zirconium alloy has the hydrogen contents which are below 30ppm at the 300 seconds experiment, but Zircaloy-4 has the hydrogen contents which are 94ppm at the 2000 seconds experiment and about 250ppm at the 3000 seconds experiment. ZIRLO shows low amount of hydrogen contents until the 2000 seconds experiment. But the hydrogen contents of ZIRLO show 108ppm at the 3000 seconds experiment. Both of Zircaloy-4 and ZIRLO are shown 1000ppm of hydrogen contents at the 5000 seconds experiment. Trend of the right graph is similar to the left one.

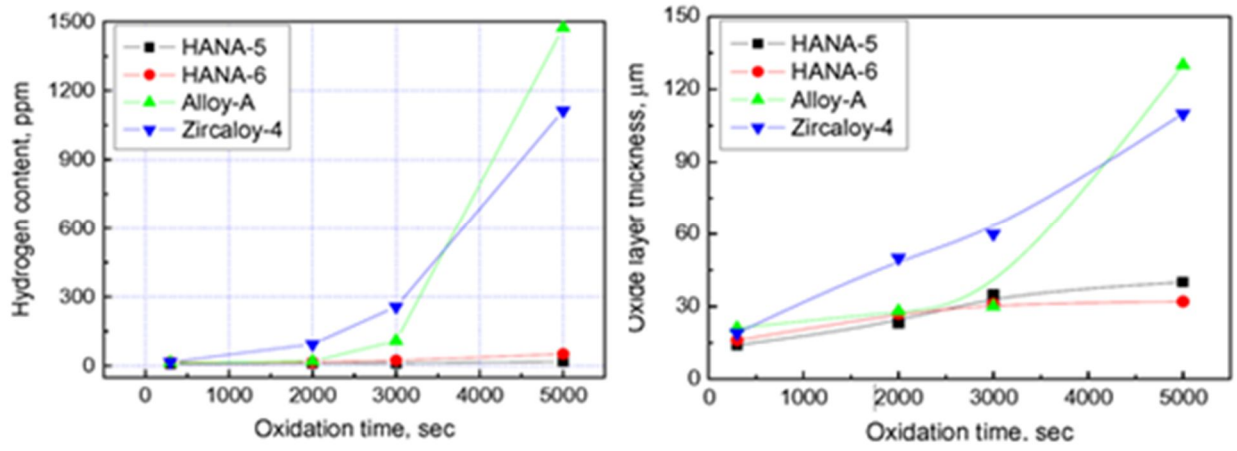

Figure II-8 The measured hydrogen content (left) and oxide layer thickness (right) of each claddings after the high temperature oxidation test [12b]

2.3 Breakaway oxidation

2.3.1 Basis of breakaway oxidation

Breakaway oxidation can be observed in the high temperature corrosion of zirconium alloy and the specimen of high temperature oxidation test has white oxide after breakaway oxidation as shown in Figure II-9. The specific condition of corrosion should be satisfied for observing breakaway oxidation, lots of factor affect breakaway oxidation phenomenon such as oxidation temperature, time, composition of zirconium alloy, fabrication method, etc [15].

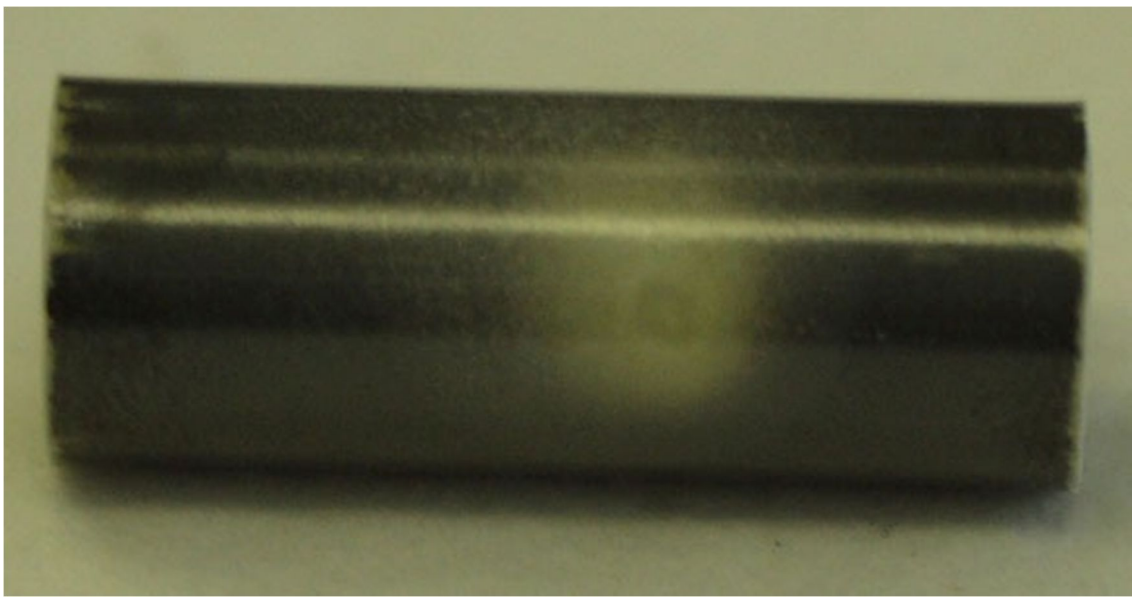

Figure II-9 White oxide on the surface can be observed after the high temperature oxidation test from conducting the test in ANL [2b]

A composition of representative zirconium alloy is introduced in the Table II-1, and the information is also introduced in the Table II-2 which is minimum breakaway oxidation time in the each alloy and

temperature when minimum time of breakaway oxidation is achieved. Zircaloy-2, 4 and ZIRLO are developed in Westinghouse, M5 is developed in France [2b, 3].

Alloy	Sn, wt.%	Nb, wt.%	Fe, wt.%	Cr, wt.%	Ni, wt.%	O, wt.%	Zr, wt.%
Zircaloy-2	1.45	-	0.14	0.10	0.06	0.125	Bal.
Zircaloy-4	1.45	-	0.21	0.10	-	0.125	Bal.
ZIRLO^{TM}	1.1	1.1	0.1	-	-	0.120	Bal.
M5	-	1.0	0.038	-	-	0.135	Bal.

Table II-1 The composition of each zirconium alloy [2b]

Alloy	Minimum Breakaway Oxidation time	Minimum Breakaway Oxidation temperature
Zircaloy-2	1,000 °C	>5,000 seconds
Zircaloy-4	986 °C	5,000 seconds
ZIRLOTM	970 °C	3,000 seconds
M5	1,000 °C	>5,000 seconds

Table II-2 The test results of breakaway oxidation test [3]

2.3.2 Breakaway oxidation mechanism

Many breakaway oxidation mechanisms had been suggested from 1970s but any theory didn't have accepted completely. The Leistikow-Schanz (LS) model is usually used to explain breakaway oxidation which is closed to the established theory [16].

Schematic of the LS model is shown as Figure II-10. Oxide layer is uniformly formed at the first time in the LS model, that oxide has a structure of tetragonal. The stress distribution and micro-crack formation is the reason why tetragonal oxide is turned into monoclinic oxide.

Because of the local formation of monoclinic oxide, a localized difference occurs in amount of produced oxide and it causes metal/oxide interface to have a wavy structure. An occurrence of a wavy structure forms the lateral crack in the oxide and the vertical crack afterward. The vertical crack accelerates absorption of hydrogen and oxygen. Finally, breakaway oxidation is occurred in zirconium alloy.

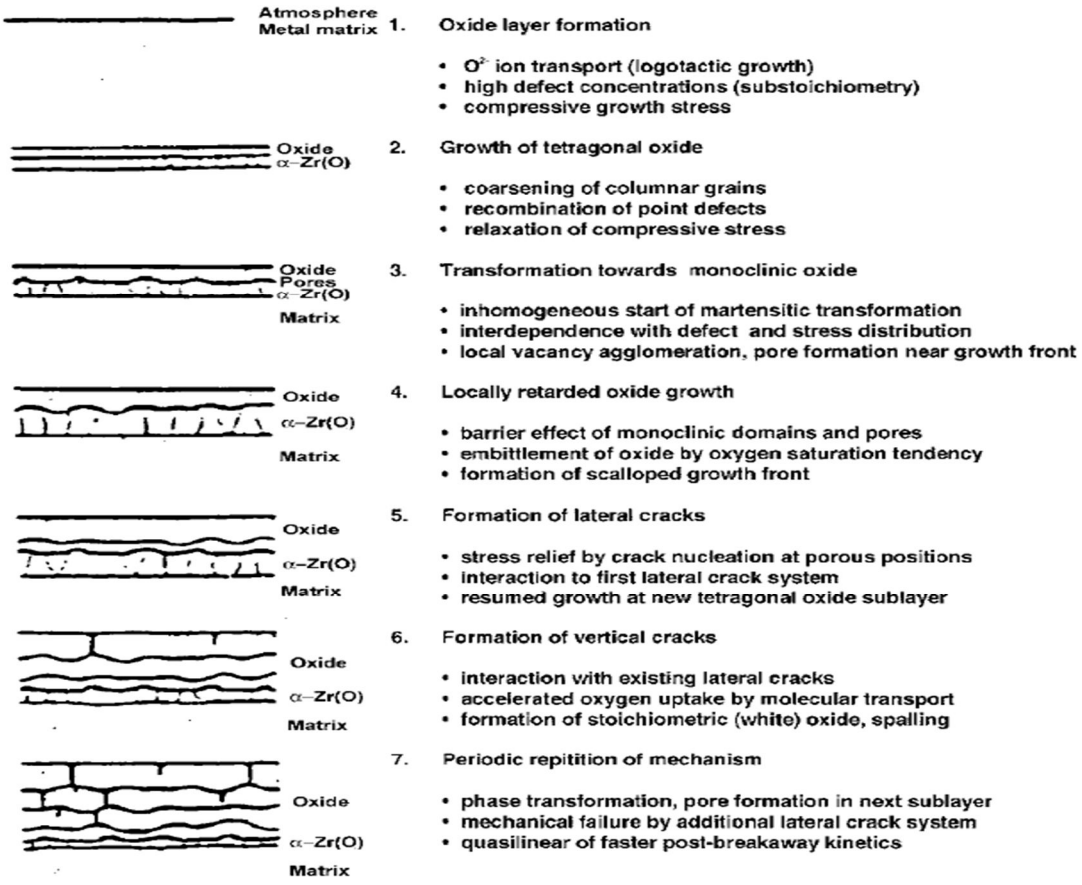

Figure II-10 Schematics of breakaway oxidation mechanism in the LS model [12b, 16]

III. Test method

The recommendation of standard test method is described in the Draft regulatory guide 1261 [3], the test method in the experiment usually follows the recommendation but some modified test procedure and equipment are used to the experiment. The following section shows the explanation of test method in the high temperature oxidation test.

3.1 Experimental equipment

3.1.1 Overall scheme of equipment

A schematic of high temperature oxidation equipment is shown as Figure III-1 and the equipment which is installed on the laboratory is shown as Figure III-2. The equipment uses the IR ramp which is used for the principle of radiation heating; this system has a benefit which can raise temperature very fast rather than other type of furnace such as electric furnace. The computer to control furnace power and temperature is installed. The panel to control electricity of furnace is attached on front of the equipment and the modules to check the conditions of furnace are also attached on the panel. The heater and insulator are installed on upper and lower torr seal for reducing droplet from condensation of steam.

The steam and water supply system is attached additionally, this system consists of the water tank, flow rate controller, steam supply equipment, etc. Argon gas for pre-purging is installed and also the computer and DAS to measure temperature.

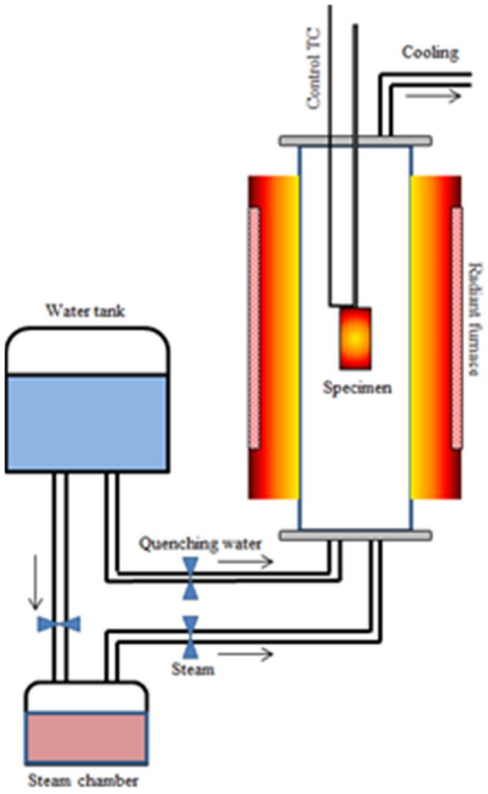

Figure III-1 Schematic of the high temperature oxidation test equipment

Figure III-2 Picture of the high temperature oxidation test equipment in the UNIST

3.1.2 Specimen cutting

8.36mm inner diameter, 9.5mm outer diameter, 4070.50mm length of ZIRLO is supplied by cladding supplier and the length of ZIRLO is cut into 40.0±1.0mm length specimen. Two cutters - ML-360 is produced by MANIX and ISOMET 5000 is produced by BUEHLER - are used for specimen cutting. ISOMET 5000 is usually used for specimen cutting because this automatic specimen cutter product doesn't need any skill to cut. ISOMET 5000 is only needed to input rotation speed (RPM), feed rate, etc. and supplier consults these factors. And the sandpaper over 1000mesh is used to remove burr on the cutting plane.

3.1.3 Specimen cleansing

The draft regulatory guide 1261 A-4.5 and ASTM G2/G2M–06 [17] introduce the cleansing method of zirconium alloy for the high temperature oxidation test, two kinds of solution are used to cleanse the specimen; alconox solution with deionized water and ethanol with acetone solution. Alconox solution is used to remove lubricating oil of ISOMET 5000, ethanol with acetone solution is used to various cleansing except immediately after cutting. Cleansing of the specimen is usually done by the ultrasonic cleaner as Figure III-3. The optimized cleansing method is introduced below;

1) After cutting

A. Put a beaker including alconox with deionized water on the hotplate until alconox powder is completely dissolved

B. Wash the specimen in the running tap water after cutting the specimen, and remove burr

C. Cleanse the specimen 20minutes on alconox solution with the ultrasonic cleaner

D. Wash the specimen in the running tap water after alconox cleansing

E. Cleanse the specimen 20minutes on 50% ethanol, 50% acetone solution with the ultrasonic cleaner

F. Blow and dry the specimen and keep on vacuum environment

2) Before experiment

A. Cleanse the specimen 5minutes on 50% ethanol, 50% acetone solution with ultrasonic cleaner

B. Blow and dry the specimen and do experiment

Figure III-3 The ultrasonic cleaner for using cleansed the specimen

3.1.4 The specimen holder

The specimen holder should be positioned on the middle of IR ramp to uniform heating and designed to reduce the steam flow resistance. The specimen holder is exposed to high temperature conditions with steam ambient like the specimen, iron based stainless steel or nickel based Inconel is usually used to the holder.

Eutectic problem is occurred when iron based or nickel based metal is attached to the zirconium alloy based specimen; local reaction can be occurred between the specimen and the holder because melting point can go down below 1000ºC. The zirconia washer and alumina holder is installed between the specimen and the holder for preventing eutectic problem in ANL. The alumina holder is also installed between the specimen and the holder in the experiment, a picture of the specimen, alumina and Inconel holder is shown as Figure III-4.

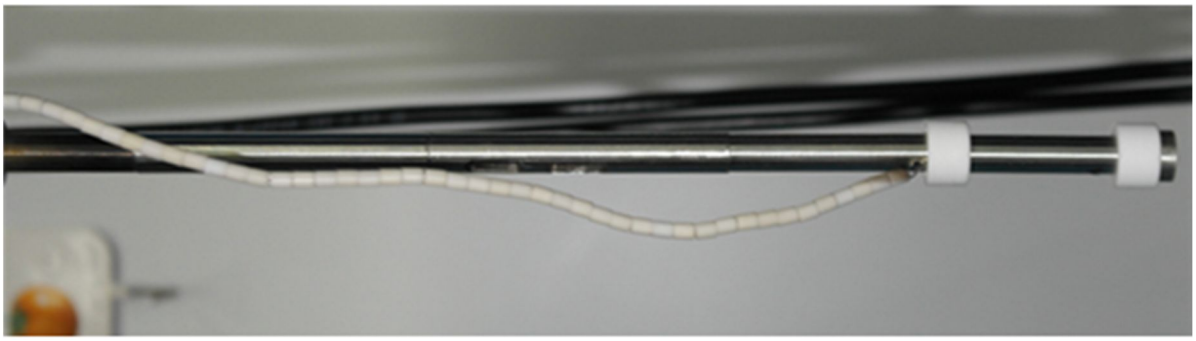

Figure III-4 The specimen holder for holding the specimen in the high temperature furnace

3.1.5 Steam supply equipment

Cladding is exposed to steam ambient become the reflood stage in the LOCA accident situation, pressure of water is decreased and vaporized to steam. The steam supply system is necessary to

provide steam which simulates steam environment and experiment should be tested in the steam flow condition. More detail contents will be provided in the chapter IV.

3.2 Experimental method

3.2.1 Purging test train

The zirconium alloy specimen can be reacted with air, especially nitrogen molecules, in the high temperature condition. This situation is critical to oxidation kinetics of specimen, so air has to be purged to leave steam only. Inert gas such as argon, helium or steam is used to purge the test train, purging time is recommended to be over 500 seconds. Steam is usually used to purge the test train in the experiment, Figure III-5 is a picture of specimen when the test train is purged in 10minutes and tested by the normal experiment procedure.

Figure III-5 Surface appearance of post-test specimen using method of steam pre-purging during 10 minutes

3.2.2 Thermocouples

Range of temperature on the experiment is maximum 1200ºC (or some experiment tested above this range) and the selection of thermocouple is recommended to K or S type thermocouples in the draft regulatory guide 1261. K type thermocouple consists of the chromel - alumel wire couple and can be applied maximum 1200ºC range. S type thermocouple consists of the platinum – 90% platinum + 10% rhodium wire couple and applied maximum 1700ºC range. R type thermocouple is similar to S type thermocouple, the improvement product of S type thermocouple consists of the platinum – 87% platinum + 13% rhodium wire couple. Thermocouple supplier said R type thermocouple is more public in recent years and more stable than S type thermocouple. R type thermocouple is used in the experiment instead of S type thermocouple. Thus, both of K type and R type thermocouple are used in the experiment.

Thermocouple is calibrated by using each K type and R type lot. The same lot of thermocouples that are the parts of an initial product was produced by the same producer with the same method, etc. Thus, one or two thermocouple is calibrated in a lot, they have very similar properties, as Table III-1.

Table III-1 shows the calibration results of K type thermocouples in the same lot, two results are almost the same as each other. The criterion in the draft regulatory guide 1261 is followed which recommend the calibration point 800ºC and 1000ºC, so the recommendation is satisfied.

Standard value (℃)	Indicated value (℃)	Corrected value (℃)
800.0	804.1	-4.1
900.0	904.3	-4.3
1000.0	1004.1	-4.1

Cetificated Number : 130606Y151
Control Number : BXA4-Y06657
Service provider : SICT
Date : 2013.06.10

Standard value (℃)	Indicated value (℃)	Corrected value (℃)
800.0	804.6	-4.6
900.0	904.9	-4.9
1000.0	1004.8	-4.8

Cetificated Number : 130606Y151
Control Number : BXA4-Y06657
Service provider : SICT
Date : 2013.06.10

Table III-1 The calibration results of K type thermocouple in the same lot

3.2.3 Temperature control

Recommended temperature control method is introduced in the draft regulatory guide 1261, and the method is shortly introduced as following; 1) increase temperature until 300ºC 2) maintain temperature 300ºC over 500seconds for stabilizing 3) increase temperature over 50ºC/s until 50~100ºC before target temperature 4) increase temperature 2~3ºC/s until target temperature 5) maintain target temperature 6) maintain steam flow until 800ºC and subsequently quench the specimen.

Figure III-6 is the graph of heating step, as mentioned before, the example of heating step with the 500 seconds isothermal oxidation condition.

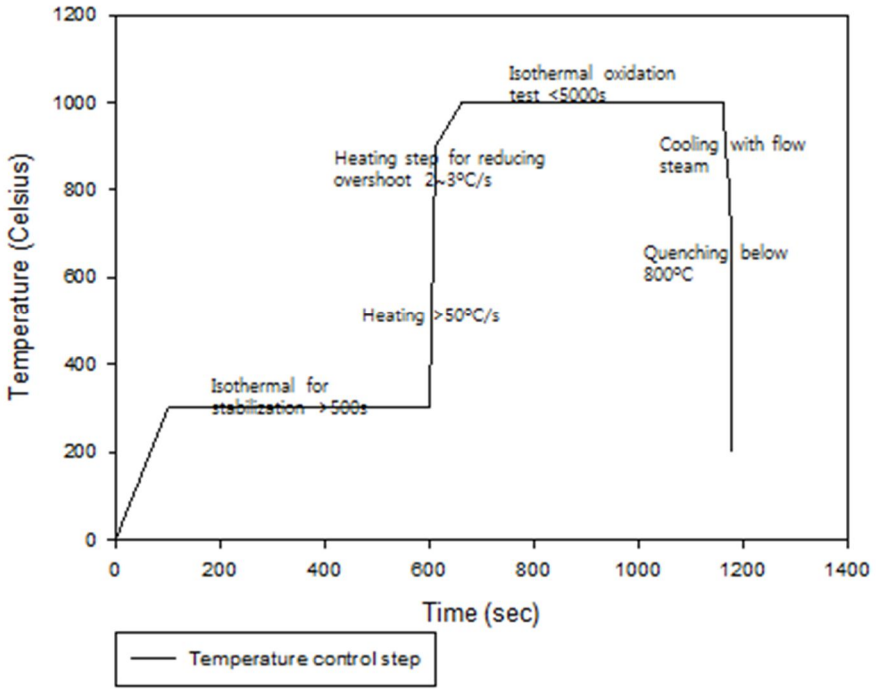

Figure III-6 Temperature control method introduced in the draft regulatory guide 1261

3.2.4 Thermal benchmark

Welding thermocouples directly onto outer surface on the specimen is not recommended, because welding can affect breakaway oxidation kinetics. The control thermocouple of furnace is used to estimate specimen temperature in the breakaway oxidation test. The identification process is named as the thermal benchmark which verifies correlation between the control TC and the specimen. The thermal benchmark is tested with the verification of temperature distribution.

3.2.5 Temperature distribution of a specimen

Uniform temperature distribution of a specimen is very important to the oxidation test, because oxidation kinetics is very sensitive to temperature. The draft regulatory guide 1261 mentions temperature distribution of a specimen as 'For a single sample, the axial temperature variation should be ≤10 ℃ and the circumferential temperature variation should be ≤20 ℃. These variations are the differences between the maximum and minimum temperatures'. The six IR ramps which are 25cm length are used to the equipment of high temperature corrosion test. The IR ramp is properly longer than a 40mm specimen and axial temperature distribution is expected to be uniform. Otherwise, axial temperature distribution is depended on the single IR ramp. Circumferential temperature distribution is depended on the each six IR ramps, it can be expected to get a worse result. But circumferential temperature distribution with the six IR ramps would have a better result than what the most of precedence work that usually applied the only four IR ramps.

Two or three thermocouples are attached to a specimen for confirming temperature distribution, as Figure III-7, the thermocouples is welded on 1/4, 2/4, 3/4 or 1/4, 2/4 point from bottom of specimen on the axial specimen. Thus, 10mm, 20mm, 30mm or 10mm, 20mm far from bottom is the point of welding for the axial specimen, the thermocouples is welded on depart from each other 120º or 180º on the circumferential specimen.

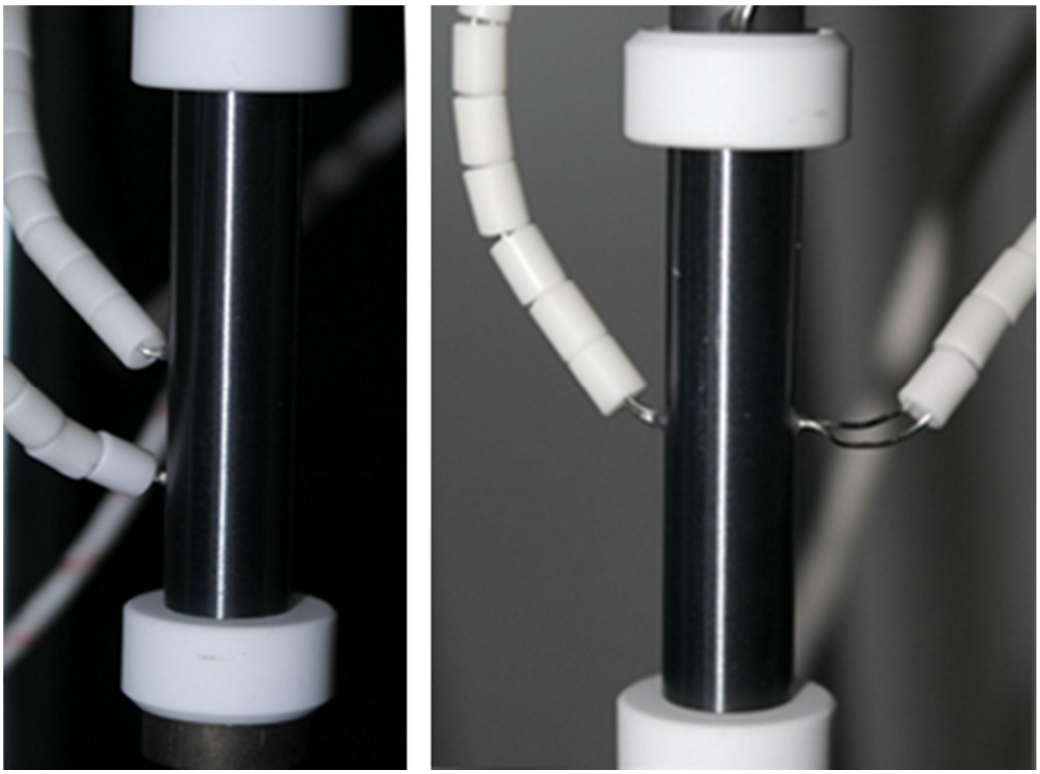

Figure III-7 The welded thermocouples to a specimen for identifying temperature distribution of a specimen

3.2.6 Weight gain benchmark

The weight gain benchmark should be tested after the thermal benchmark for confirming the result of thermal benchmark. The draft regulatory guide 1261 suggests that the result of the weight gain benchmark should be checked with the Cathcart-Pawel (CP) – ECR correlation. The CP-ECR correlation is as following [18];

$$W_g = 0.602\ exp\left(-\frac{10050}{T}\right) t^{1/2}$$

$$\mathrm{ECR} = 43.9\frac{\frac{W_g}{h}}{\left(1-\frac{h}{D_0}\right)}$$ for one side oxidation test

$$\mathrm{ECR} = \frac{87.8W_g}{h}$$ for two side oxidation test

Abbreviation :

**** Wg : weight gain per area, g/cm²***

**** K : Arrhenius Equation***

**** T : Temperature, K***

**** t : Time, seconds***

**** Q : Constant***

**** R : Universal gas constant***

**** ECR : Equivalent Cladding Reaction, %***

**** h : Zr alloy height, cm***

**** Do : Zr alloy OD, cm***

If the experimental weight gain isn't ranged within ±10% of the CP correlation, the thermal benchmark should be tested again in the guideline. The weight gain benchmark is recommended on the 800ºC and 1000ºC test, but the vendor-generated database or the results that had given in NUREG/CR-6967 [2b] should be used to the 800ºC test because the CP correlation can be applied above 1000ºC.

IV. Install a new steam supply equipment

4.1 Problem of initial steam supply equipment

As mentioned above, the steam supply equipment should be equipped to the test train for providing steam condition. The initial steam supply equipment has a twisted long pipe in the system and the heated pipe gives heat to the running water for supplying steam. But the initial steam supply equipment has a problem which is observed periodic transient of the equipment. Temperature on the system is varied up and down periodically, and steam flow rate is sharply increased when temperature on the system is increased. Periodic transient is observed as following;

1. Normal state
2. Sharply increase steam flow
3. Subsequently, temperature of the steam supply equipment is decreased about 50~100ºC (300ºC→200~250ºC)
4. Increased steam flow and low temperature is maintained for a minute.
5. Return to the normal state, and repeat the process every 5~10 minutes

Supplement water is used by the thin pipe of water in the initial steam supply equipment that is expected to cause periodic transient. Thus, the steam supply equipment is changed into the chamber type, the new steam supply equipment have the own water tank as shown in Figure IV-1. Before and after changing the steam supply equipment is shown as Figure IV-2. The initial steam supply equipment is the continuous reactor concept. Changing temperature of a steam pipe is the method of power control. But the new steam supply equipment is like the batch reactor, the steam chamber is heated to supply steam and the control of electricity input is the control method of power. The process

of new equipment installation, the measurement of steam flow rate will be shown in the following chapter.

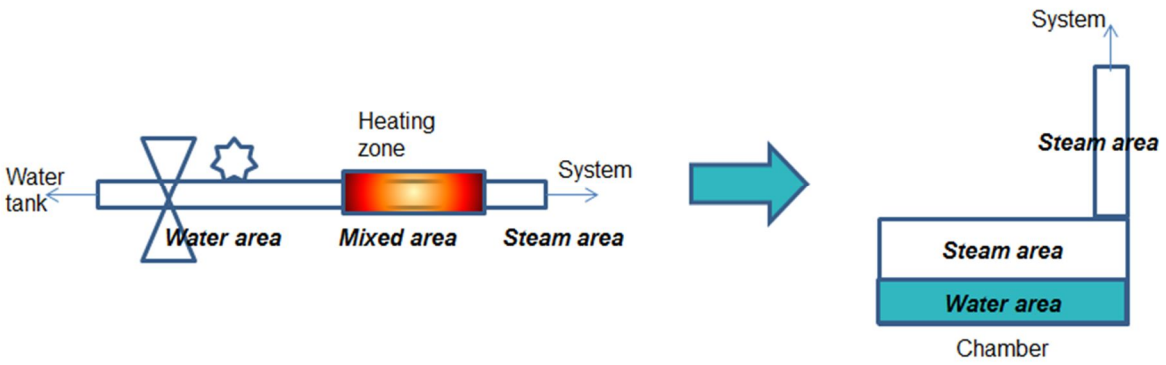

Figure IV-1 Schematic of the steam supply equipment

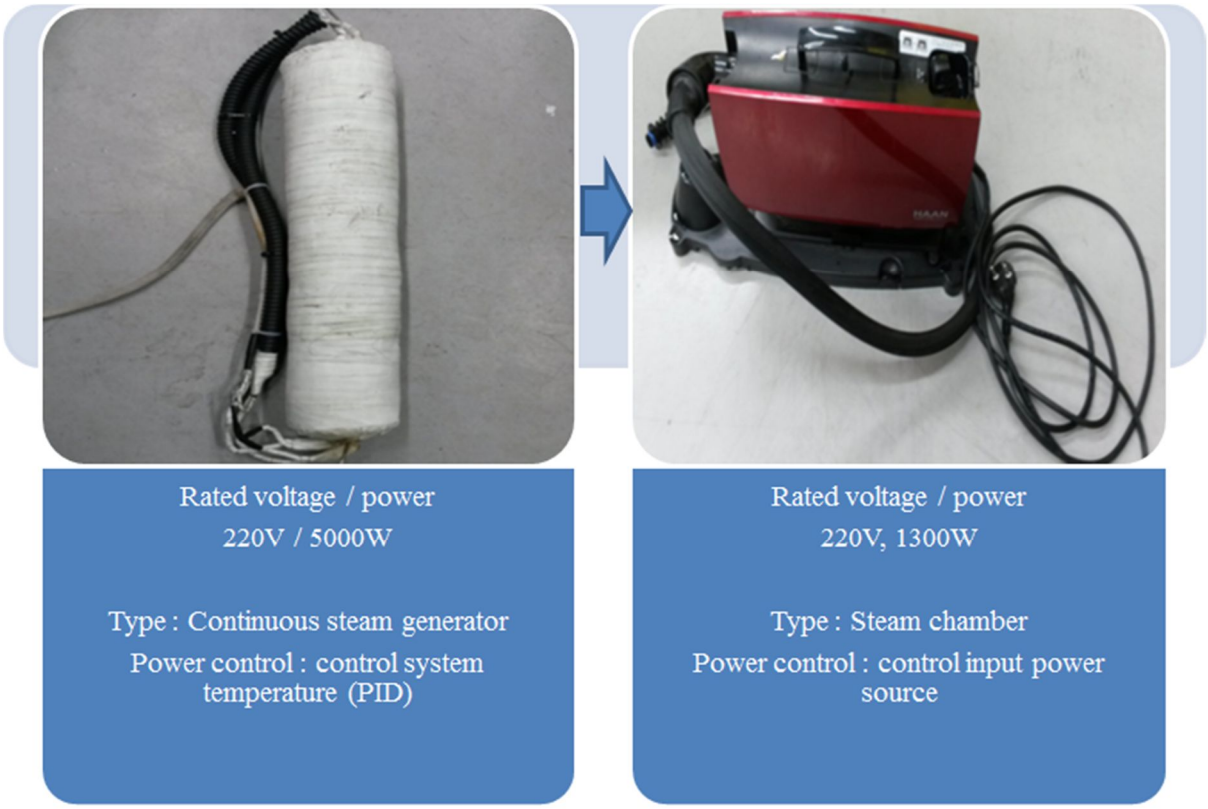

Figure IV-2 Picture and specification of the steam supply equipment

4.2 Install the new steam supply equipment

The connection method is prepared by using the PVDF connector between the steam supply equipment and high temperature furnace system. The problem is appeared because over the new steam supply equipment that doesn't use a standard size. The steam line is flexible hose which is about 22mm+α OD, 15mm+α ID. This flexible hose has elasticity, thus the size of hose is marked variable size. Stretching the hose is easier than compressing the hose, 1 inch (25.4mm) OD and 3/4 inch (19.05mm) IDs which are bigger than a normal size of flexible hose, are used as a standard.

The PVDF connector is supplied by lk lab korea, C20-140-516 (Reduction Straight Connector). C20-140-516 is the reduction connector 3/4 inch (19.05mm) to 1/2 inch (12.70mm), the steam supply equipment is linked with the 3/4 inch part and the furnace system is linked with the 1/2 inch part. The 3/4 inch part is inserted in the stretched flexible hose with covering vacuum grease, and fixed by the stainless bands and cable ties. The ferrule set is inserted in the 1/2 inch part for fastening pipe and the metal side of pipe is covered by the heater for preventing condensation of steam.

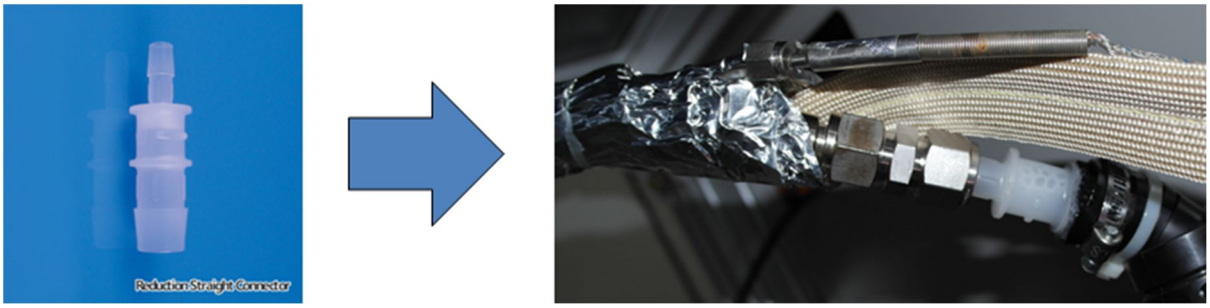

Figure IV-3 The PVDF connector which is used to the experiment supplied by lk lab

There are additional problem that the new steam supply equipment doesn’t have the own power control method. The electrical power controller is prepared to control the steam supply equipment which is named as slidacs (voltage transformer). Slidacs is produced by inparo company and voltage

can be varied easily. Power can control by turning the handle on the top. Power variation can be observed by the analog panel.

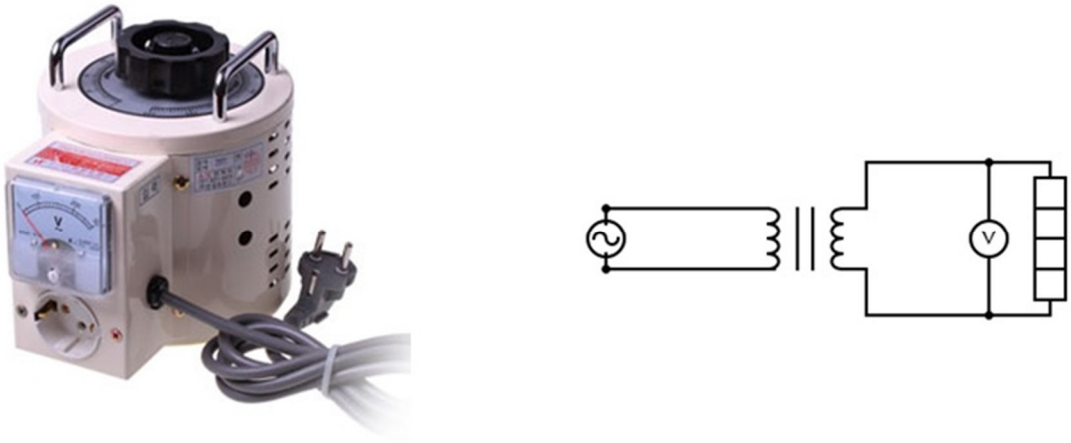

Figure IV-4 Picture of slidacs (left) and circuit of slidacs and the steam supply equipment (right)

Specification	Value
Input voltage	220V
Output voltage	0~240V
Maximum power	3000VA

Table IV-1 Specification of slidacs

4.3 Theoretical steam generation rate

Heat of vaporization from water to steam is 2260J/g at 1atm, 373K in the literature survey [19]. If heat is supplied P J/s (W) to 373K water in adiabatic environment, steam generation rate would be as the following.

$$\text{Steam generation} = \frac{\text{P (J/s)}}{2260\ (J/g)} = \frac{P}{2260}(g/s) = \frac{P}{37.67}(g/min)$$

The recommendation of steam flow rate is 0.5 ~ 30 mg/cm^2·s [3], so steam generation rate should be converted to generation rate per unit area. Cross sectional area of quartz tube is about 23.76cm^2 (Inner diameter = 5.5cm), the result of conversion is as following;

$$\text{Steam generation per unit area} = \frac{\text{P}}{37.67}(g/min) \times 1000(mg/g) \times \frac{1}{60}(min/s) \times \frac{1}{23.76}(/cm^2)$$
$$= 0.019 * \text{P (mg/cm}^2 \cdot s)$$

Maximum steam generation is 24.7 mg/cm^2·s (35g/min) when power is 1300W which is maximum power of the steam supply equipment. Of course, this maximum steam generation isn't achieved because of heat loss, efficiency of transformer, etc. But steam generation is expected to take proper range of the recommendation, the criterion will be satisfied.

4.4 Measurement of steam flow rate

The plate-type heat exchanger is used to measure steam flow rate in the left side of Figure IV-5, principle of plate-type heat exchanger is what the primary side is cooled by coolant of secondary side. The water line which is very thin is spread like the mesh for maximizing surface area, like right side of Figure IV-5. This plate-type heat exchanger, named as DSB 193-11F, is produced by Daesung engineering company.

The entrance of secondary side is connected with the faucet of tap water, tap water is circulated and cooling the primary side. Steam is entered into the entrance of primary side and emitted to the exit of primary side as water. Output water is measured every 5 minutes and this process is repeated until 30 minutes for each voltage of slidacs. If one set is finished, the experiment would be repeated by changing power.

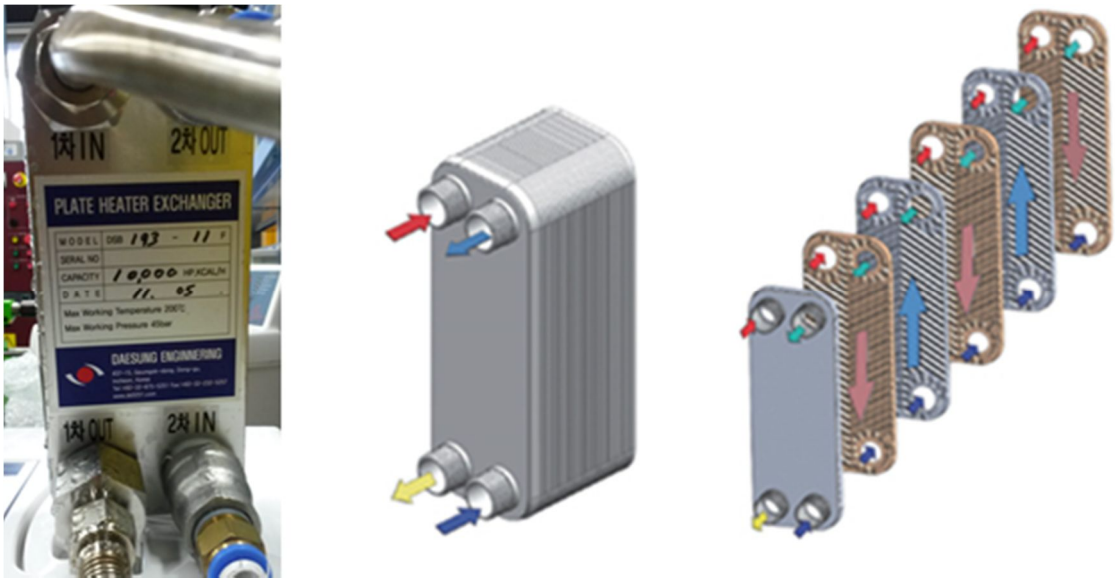

Figure IV-5 Picture and cross-sectional view of the plate type heat exchanger for measuring steam generation rate (Homepage of company, http://www.ds5251.com/)

Table IV-2 and Figure IV-6 are the results of steam flow rate measurement when slidacs is used in experiment. Flow rate 4~30ml/min is range of voltage within 100~220V. Steam flow rate 4ml/min is matched with 100V and 20ml/min is matched with 186V which is calculated by the interpolation method between 180V and 200V. The graph is dealt with mid-point flow rate ± range of data.

Voltage (V)	Minimum flow rate (ml/min)	Maximum flow rate (ml/min)	Mid-point flow rate (ml/min)
220	30	30	30
200	25	25	25
180	16	20	18
160	14	16	15
140	10	12	11
120	6	8	7
100	4	4	4

Table IV-2 Variation of steam flow rate according to voltage of slidacs

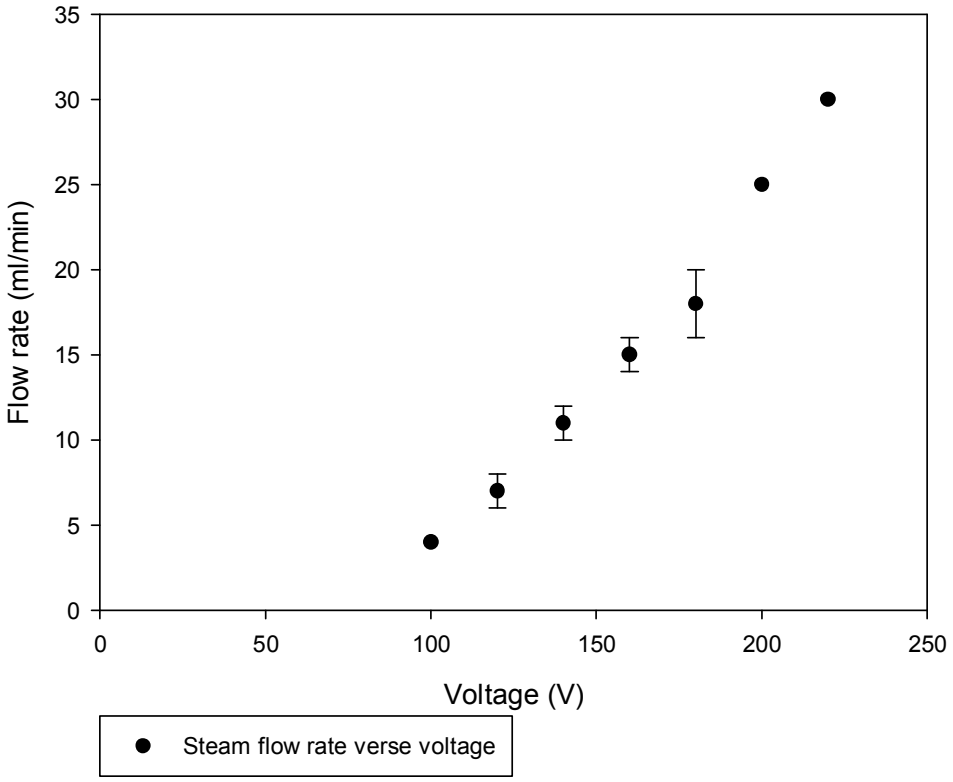

Figure IV-6 Variation of steam flow rate according to voltage of slidacs

V. Results of high temperature oxidation test

5.1 Axial and circumferential temperature distribution in a specimen

As mentioned before, temperature distribution in a specimen is the one of recommendations in the test guideline. Temperature distribution for each axial and circumferential direction is measured by the thermocouples with welded on a specimen.

The K or R type thermocouples are welded on a specimen for axial or circumferential direction. The two or three thermocouples are welded axially on location of 10mm and 20mm or 10mm, 20mm and 30mm height from bottom of a specimen, circumferentially on location of opposite direction with middle of a specimen. The specimens which were used to measure temperature distribution are shown as Figure V-1, each pictures are the specimen for the axial and circumferential measurement.

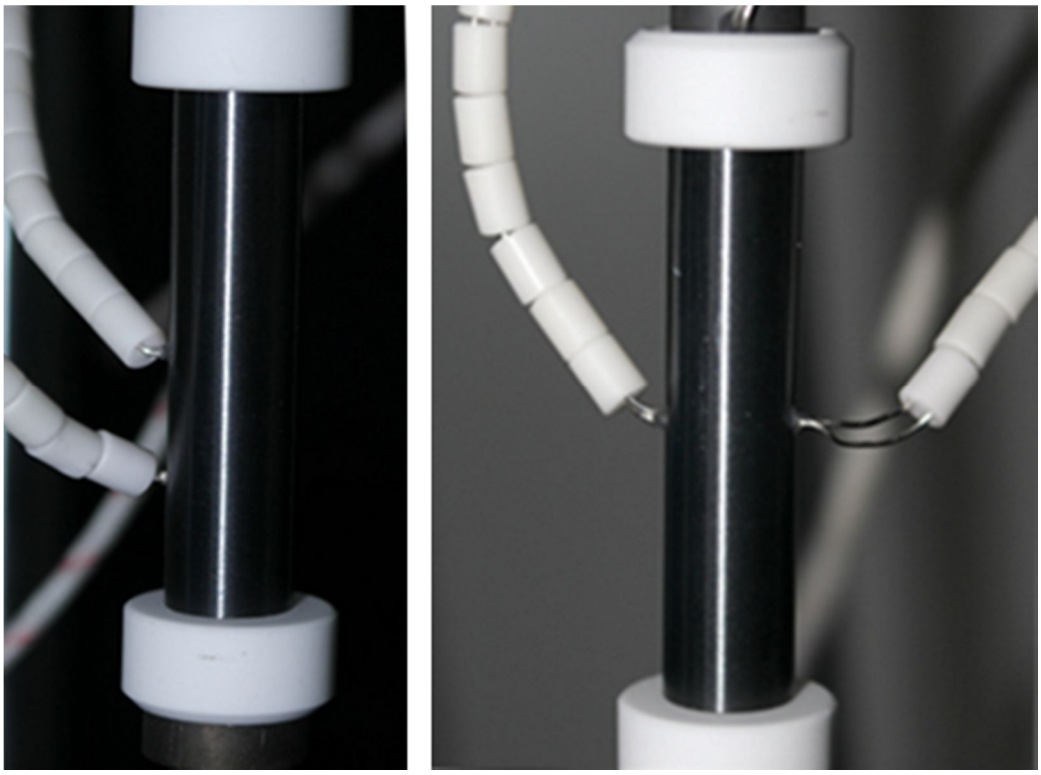

Figure V-1 The specimens for measuring temperature difference axially and circumferentially

5.1.1 Axial temperature distribution

The results of measurement of axial temperature distribution in a specimen are shown in Table V-1. Temperature difference between 10mm and 20mm from bottom of a specimen is measured when the control TC is set on 879ºC and 1077ºC.

Control TC (ºC)	10mm from bottom (ºC)	20mm from bottom (ºC)	Difference (ºC)
879	866	863	3
1077	1069	1069	0

Table V-1 The results of axial temperature difference measurement

Temperature differences between two point are 3ºC when the control TC are set on 879ºC, and 0ºC when the control TC are set on 1077ºC. As mentioned before, the recommendation of axial temperature difference is lower than 10ºC, the results are satisfied the criterion.

5.1.2 Circumferential temperature distribution

The results of measurement of circumferential temperature distribution in a specimen are shown in Table V-2. Temperature difference between opposite direction of a specimen is measured when the control TC is set on 879ºC and 1077ºC.

Control TC (ºC)	Left (ºC)	Right (ºC)	Difference (ºC)
879	875	882	7
1077	1087	1084	3

Table V-2 The results of circumferential temperature difference measurement

Temperature differences between two point are 7ºC when the control TC are set on 879ºC, and 3ºC when the control TC are set on 1077ºC. As mentioned before, the recommendation of circumferential temperature difference is lower than 20ºC, the results are satisfied the criterion.

5.2 Comparison of the weight gain

The results of weight gain measurement are compared with the well-established data which is measured by Westinghouse [20] and Argonne National Laboratory [2b]. The weight gain data is shown as the Cathcart-Pawel (CP) predicted weight gain in x axis and the measured weight gain in y axis.

The results of weight gain measurement are shown as Figure V-2, there are very similar trends of weight gain results. All of the data have the lower measured weight gain than the CP predicted, and the weight gain results are consistent with the well-established data.

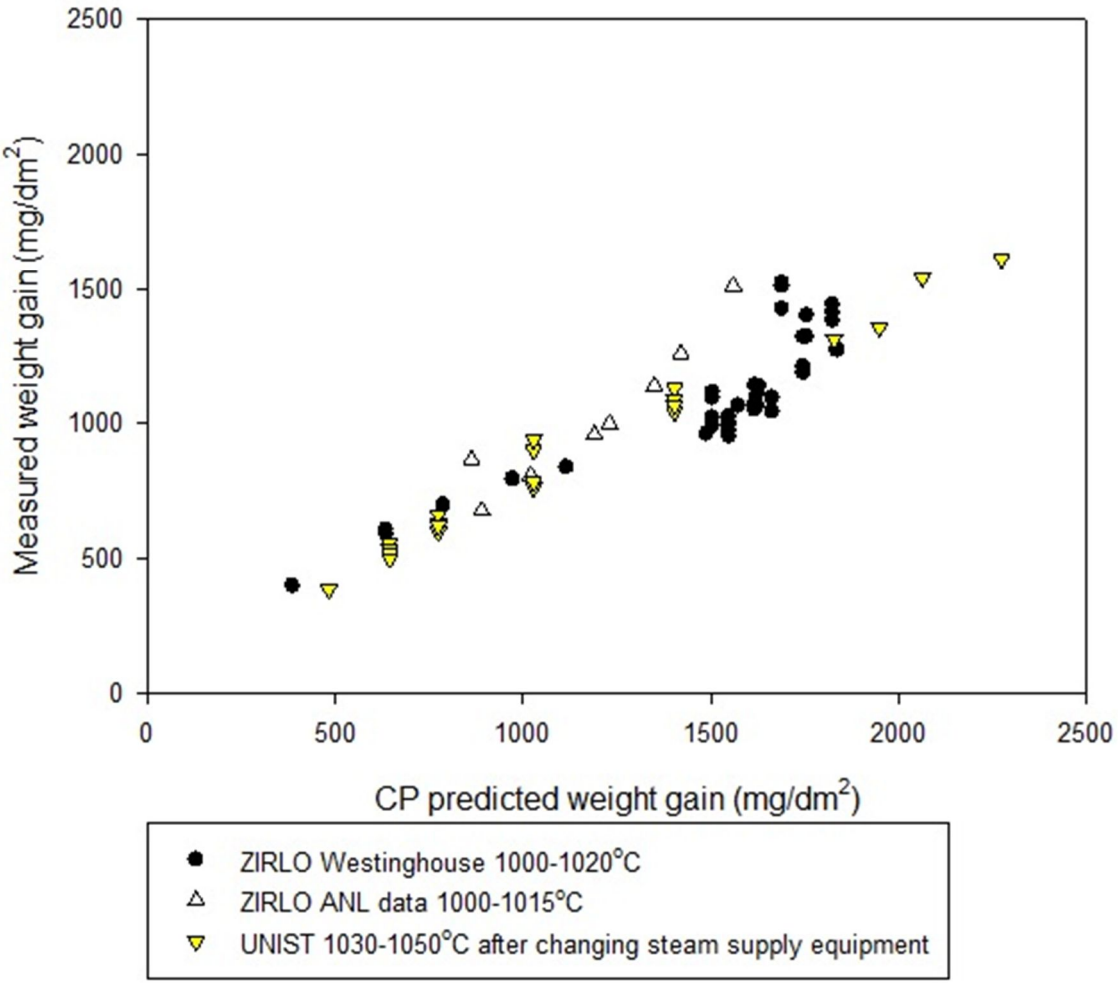

Figure V-2 Results of the weight gain measurement compared with the test results of Westinghouse and ANL [2b, 20]

5.3 Surface condition after high temperature oxidation test

The observation results of specimen appearance of ZIRLO after the high temperature oxidation are shown in the Figure V-3. As-fabricated ZIRLO is seemed like silver color and lustrous black can be observed after the high temperature oxidation. Lustrous black surface is transformed to white oxide on local region.

Figure V-3 Specimen appearance after the high temperature oxidation in order of time

5.4 Microstructure

The microstructure of ZIRLO after the high temperature oxidation is shown as Figure V-4 and Figure V-5. Oxidation time of microstructure in the Figure V-5 is longer than oxidation time of the microstructure in the Figure V-4. Metal / oxide interface is focused on the analysis of the

microstructure in the following because the transition from flat to wavy interface between metal and oxide is the precursor to breakaway oxidation in the LS model [16]. The next stage of wavy interface is circumferential and axial crack of oxide, circumferential oxide is formed in advance.

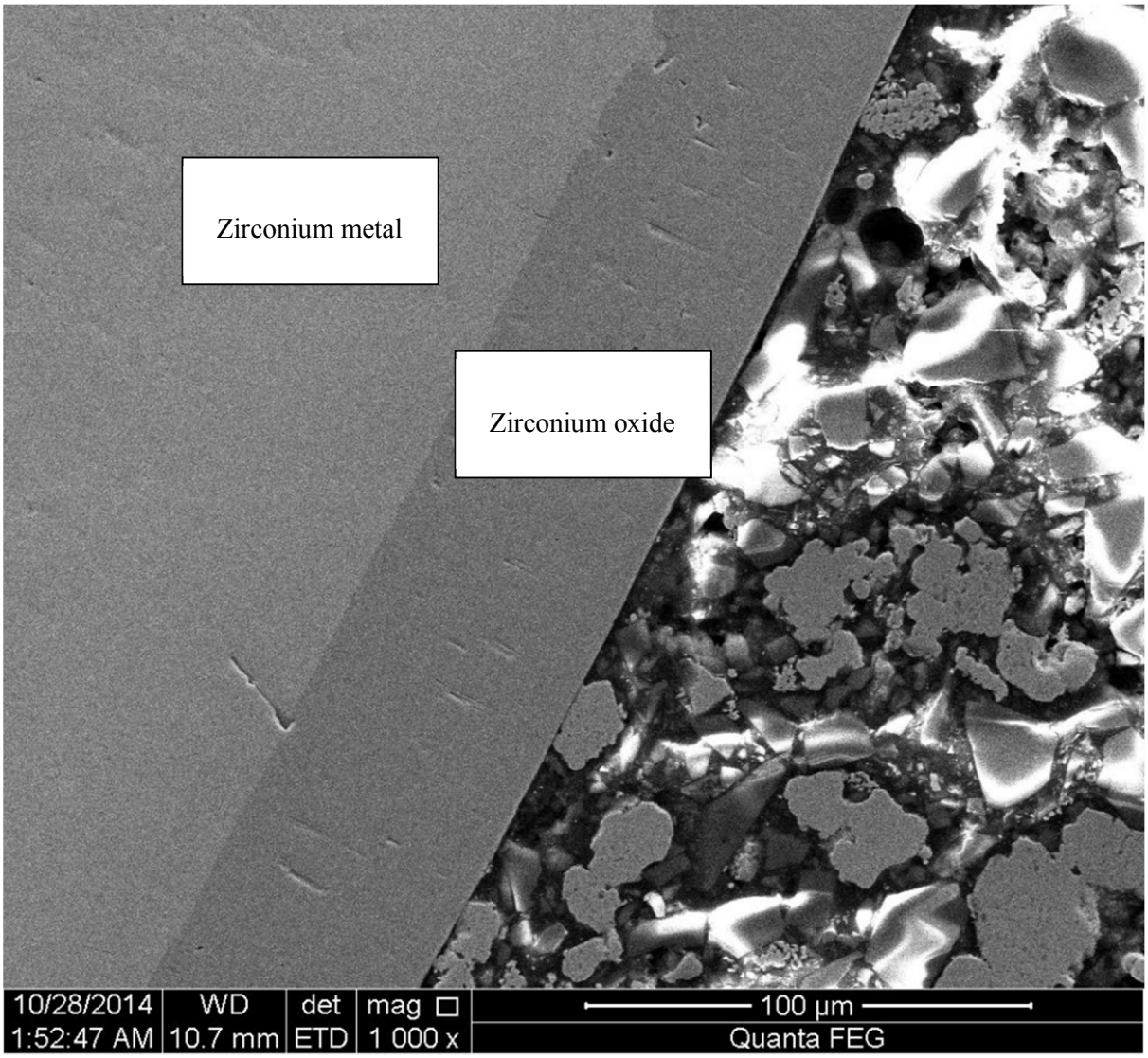

Figure V-4 The microstructure of ZIRLO specimen which is shown as flat interface between metal and oxide

The microstructure of a specimen when the measured weight gain is about 2458mg/dm^2 is shown as Figure V-4. Metal / Oxide interface is flat interface in the specimen, the precursor to breakaway oxidation isn't observed in the Figure V-4.

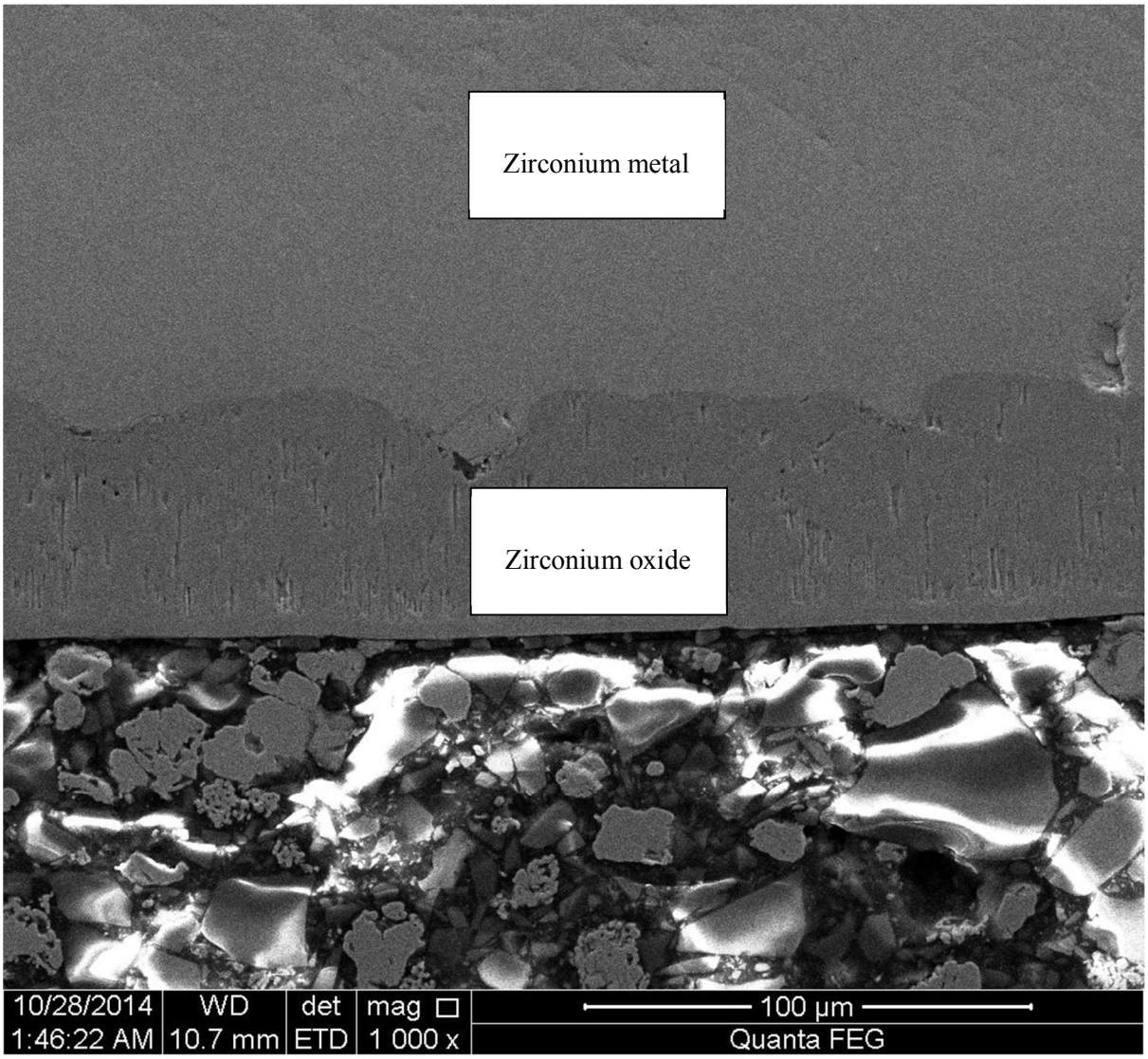

Figure V-5 The microstructure of ZIRLO specimen which is shown as wavy interface between metal and oxide

The microstructure of a specimen when the measured weight gain is about 3002mg/dm^2 is shown as Figure V-5. Metal / Oxide interface is wavy interface in the Figure V-5, the precursor to breakaway oxidation is observed in the Figure V-5.

VI. Conclusion

High temperature oxidation test have been performed for the test of breakaway oxidation, the high temperature oxidation equipment was set up following the recommended guideline, which is suggested by U.S NRC, the draft regulatory guide 1261.

The initial steam supply equipment showed the unstable steam flow and the unstable steam flow is occurred probably because of the water supply system of the initial steam supply equipment. So that, the new steam supply equipment is changed to the chamber type and that doesn't show the unstable steam supply. The stable steam flow is expected to generate credible data for the high temperature oxidation test. Furthermore, steam generation of the new steam supply equipment was measured by the plate-type heat exchanger and the data of steam generation will be used to conduct the high temperature oxidation test.

The verification tests for the high temperature oxidation test are progressed, axial temperature distribution shows under 3ºC and circumferential temperature distribution shows less than 7ºC. Temperature distribution in a specimen is satisfied with the recommendation and that is expected to maintain the uniform heating on a specimen for the high temperature oxidation test.

The results of ZIRLO weight gain measurement are consistent with the well-established data by Westinghouse and ANL. Flat interface between the metal and oxide is observed in the early period of the high temperature oxidation test, but wavy interface between the metal and oxide is observed after the breakaway oxidation; flat to wavy transition of the interface was reported to be the precursor of the breakaway oxidation by other authors. Thus, the high temperature oxidation test of the ZIRLO tube has been performed successfully.

References

1. 10 CFR Parts 50 and 52, RIN 3150–AH42, Performance-Based ECCS Acceptance Criteria; Proposed Rule. USNRC, Federal Register: 2014.

2. (a) Hache, G.; Chung, H. In *The history of LOCA embrittlement criteria*, 28th Water Reactor Safety Information Meeting, 2001; pp 205-237; (b) Billone, M.; Yan, Y.; Burtseva, T.; Daum, R. *Cladding embrittlement during postulated loss-of-coolant accidents*; Argonne National Laboratory (ANL): 2008.

3. Conducting Periodic Testing For Breakaway Oxidation Behavior, Draft Regulatory Guide DG-1261. USNRC: 2011.

4. Testing For Postquench Ductility, Draft Regulatory Guide DG-1262. USNRC: 2011.

5. Establishing Analytical Limits For Zirconium-Based Alloy Cladding, Draft Regulatory Guide DG-1263. USNRC: 2011.

6. Allen, T. R.; Konings, R. J. M.; Motta, A. T., 5.03 - Corrosion of Zirconium Alloys. In *Comprehensive Nuclear Materials*, Editor-in-Chief: Rudy, J. M. K., Ed. Elsevier: Oxford, 2012; pp 49-68.

7. Adamson, R.; Garzarolli, F.; Cox, B.; Strasser, A.; Rudling, P., Corrosion mechanisms in zirconium alloys. *ZIRAT r2 special topic report corrosion mechanisms in zirconium alloys* **2007**.

8. Lemaignan, C., 2.07 - Zirconium Alloys: Properties and Characteristics. In *Comprehensive Nuclear Materials*, Editor-in-Chief: Rudy, J. M. K., Ed. Elsevier: Oxford, 2012; pp 217-232.

9. Nagase, F., 2.23 - Behavior of LWR Fuel During Loss-of-Coolant Accidents. In *Comprehensive Nuclear Materials*, Editor-in-Chief: Rudy, J. M. K., Ed. Elsevier: Oxford, 2012; pp 595-608.

10. Anghel, C. Studies of transport in oxides on Zr-based materials. Licentiate thesis, comprehensive summary (Other scientific), Royal Institute of Technology, KTH, Stockholm, 2004.

11. Reed, T. B., *Free energy of formation of binary compounds*. MIT press: 1971.

12. (a) Aomi, M.; Nakatsuka, M.; Komura, S.; Hirose, T.; Anegawa, T. In *Behavior of BWR fuel cladding tubes under simulated LOCA conditions*, 7th International Conference on Nuclear Engineering, ICONE-7435, 1999; (b) Kim, H.-G.; Kim, I.-H.; Choi, B.-K.; Park, J.-Y., A study of the

breakaway oxidation behavior of zirconium cladding materials. *Journal of Nuclear Materials* **2011,** *418* (1–3), 186-197; (c) Kim, H. H.; Kim, J. H.; Moon, J. Y.; Lee, H. S.; Kim, J. J.; Chai, Y. S., High-temperature Oxidation Behavior of Zircaloy-4 and Zirlo in Steam Ambient. *Journal of Materials Science & Technology* **2010,** *26* (9), 827-832.

13. Park, D. J.; Park, J. Y.; Jeong, Y. H.; Lee, J. Y., Microstructural characterization of ZrO2 layers formed during the transition to breakaway oxidation. *Journal of Nuclear Materials* **2010,** *399* (2–3), 208-211.

14. Steinbrück, M., Hydrogen absorption by zirconium alloys at high temperatures. *Journal of Nuclear Materials* **2004,** *334* (1), 58-64.

15. Ahmed, T.; Keys, L. H., The breakaway oxidation of zirconium and its alloys a review. *Journal of the Less Common Metals* **1975,** *39* (1), 99-107.

16. Leistikow, S.; Schanz, G., Oxidation kinetics and related phenomena of zircaloy-4 fuel cladding exposed to high temperature steam and hydrogen-steam mixtures under PWR accident conditions. *Nuclear Engineering and Design* **1987,** *103* (1), 65-84.

17. ASTM, G2/G2M-06 Standard Test Method for Corrosion Testing of Products of Zirconium, Hafnium, and Their Alloys in Water at 680°F (360°C) or in Steam at 750°F (400°C). In *G2/G2M-06*, ASTM International: 2011.

18. Cathcart, J.; Pawel, R.; McKee, R.; Druschel, R.; Yurek, G.; Campbell, J.; Jury, S. *Zirconium metal-water oxidation kinetics. IV. Reaction rate studies*; Oak Ridge National Lab., Tenn.(USA): 1977.

19. Cengel, Y. A.; Boles, M. A.; Kanoğlu, M., *Thermodynamics: an engineering approach*. McGraw-Hill New York: 2011; Vol. 5.

20. Westinghouse, *Weight Gain Data for Zircaloy-4 and ZIRLO Breakaway Tests (Non-Proprietary)*; LTR-NRC-11-10 NP-Attachment: 2011.

Acknowledgments

길다고 하면 길수도 있고, 짧다고 하면 짧을 수도 있는 2 년간의 석사 과정이 마지막에 도달했습니다. 제 인생에서 가장 많은 것이 바뀌고, 많은 것을 하였던 2 년이 끝나간다고 생각하니 아쉽기도 하고, 설레기도 하고, 기쁘기도 하고, 슬프기도 합니다. 학사 학위부터 6 년간 이 학교에서 머무르며 생활하였는데, 이번 졸업 후 정든 울산과 이 학교를 떠야 된다는 사실이 아직도 믿기지 않습니다. 이번 2 년간 힘든 일도 많이 있었고, 학위 과정을 중도 하차하고자 하는 상황까지도 갔었으나, 결국 이렇게 졸업 논문을 낼 수 있다는 사실이 감개무량합니다. 이에 마지막으로 지금까지 제게 도움을 준 많은 분들에게 감사하고자 이 글을 바칩니다.

먼저 제가 어떤 선택을 하든 존중하고, 적극적으로 도와주신 제 부모님께 감사의 말씀을 올리고 싶습니다. 학위 도중 집안의 우환이 있어 다소 문제가 있기도 했었지만, 학위 과정을 무사히 잘 마칠 수 있었습니다.

또한 학부 4 학년때부터 약 3 년간 지도해주신 저희 손동성 교수님께도 감사의 말씀을 올리고 싶습니다. 모자란 저를 잡아주시고 끝까지 잘 이끌어 주셔서 감사합니다. 지금까지 포기하지 않으시고 많은 것을 알려주신 가장 고마운 분들 중 한 분이십니다.

또한 이 실험을 하며 생겼던 여러 문제를 같이 논의하고 해결하며 도와주고, 서로 웃고 울며 2 년간 살아온 실험실 전체, 조병진 형, 조태원, 김지현 누나, 정관윤, 이철민, 김미진, 그리고 이희재에게 감사의 말씀을 올리며, 뿐만 아니라 지금은 여기 없지만 이

실험을 했었던 김영진 형, 이주영 누나, 이외에도 실험실을 거쳐간 많은 학생들이 생각납니다.

또한 학부 때부터 많은 것을 가르쳐주신 방인철 교수님, 김지현 교수님, 이덕중 교수님, 김희령 교수님과 직, 간접적으로 도움을 주신 김연수 박사님께도 감사의 말씀을 올립니다.

이외에도 지금 재학중인, 혹은 졸업한 많은 원자력공학과 대학원생들, 같은 자연과학관 406 호를 사용한 재료 실험실의 신상훈 형, 김종진 형, 최경준 형, 최상일 형, 김태호 형, 김승현 형, 고광범, 이정현, 유승창. 지금은 아니지만 406 호를 같이 쓴 방사선 실험실의 유동한 형, 김건희, 이욱제, 곽재식, 배준우. 학부생 시절 몸 담았었던 열수력 실험실의 이승원 형, 박성대 형, 강사라 누나, 김성만 형, 서한 형, 김경모, 김인국, 문성보, 서석빈, 정영신, 허효. 5 층에 있어서 자주 만나기가 힘든 노심 실험실의 탁태우 형, 이현석 형, 최수영, 공치동, 최지원, 모두가 같이 했었던 것도 나중에는 추억으로 남을 일일 테지요.

이외에도 학교 내외로 정말 많은 친구, 선배, 후배들 모든 분들에게 감사의 말씀을 올립니다. 많은 사람들을 만나며 직, 간접적인 도움을 많이 얻었던 것 같습니다. 모든 분들이 건강하게 다시 만날 수 있었으면 좋겠습니다.